

Article

The photochemical Catalytic Properties and Hydrothermal Synthesis of Magnesium Borate for Efficient Removal of Congo red dye from Aqueous Solution.

Hasan Jasim Mohammed and Zaki N. Kadhim

Chemistry Department, College of science University of Basra. IRAQ.

zaki.kadhim@uobasrah.edu.iq , Jasiem33@gmail.com

Abstract

In this study, Magnesium Borate (MB) ,was synthesized by one step precipitation from nano Magnesium oxide and Boric acid. The product was characterized by FTIR, XRD, SEM, EDX and Zeta potential. This product act as photocatalyst to remove Congo red dye (CR) from aqueous solution, all factors that effect on adsorption process studied (Time, weight of adsorbent, adsorbate concentration, pH, temperature). Model of isotherm adsorption Langmuir and Freundlich, kinetic adsorption, first order and second order pseudo and values of thermodynamic (ΔS , ΔG , ΔH) are studied. Results of study indicated that best amount of adsorbent was 0.1 g used against dye, optimal concentration of CR was 50 mg L^{-1} , and optimum acidity function was equal to 5.5 with a volume of 100 ml. Adsorption processes were carried out using distilled water as solvent. Also, this study included calculating adsorption capacity based on optimal conditions that were obtained by applying Langmuir and Freundlich isotherm models, and $q_{\text{max}} = (222.2) \text{ mg g}^{-1}$ for (MB), kinetic adsorption following second order pseudo .Values of thermodynamic (ΔS , ΔG , ΔH) are measured and the results indicating increase in system randomness and that adsorption process is spontaneous and endothermic.

Key Words : Magnesium borate, Congo Red dye, Adsorption

1.Introduction

Magnesium borates famous material traditionally needs for their strong mechanical and thermal features due to their high elasticity coefficient, corrosion, heat resistance, and high surface area⁽¹⁾. Magnesium borates (MB) is continuously produced and used for various applications in industry due to their specific properties e.g., a flame retardant⁽²⁾, corrosion inhibitors, smoke suppressant, synergistic effect, good mechanical properties, and high surface area due to these characteristic features, different types of magnesium borates can be used in various areas⁽³⁾, including the thermo-luminescent phosphors, catalysts for hydrocarbon conversions, , wide band gap semiconductors matrixes. Dyes are colored substances that have the ability to transfer their distinctive colors to materials to be dyed⁽⁴⁾. CR dye belongs to the class of industrial dyes from azo family because it contains azo groups linked to aromatic rings in its structure. This dye is distinguished by its intense color and chemical stability against influencing factors. It is of many types, as it represents 60-70 % of all dyes. The presence of CR dye in wastewater in different concentrations is a source of major environmental pollution that must be treated through various methods used to treat wastewater⁽⁵⁾. There are many methods and theories used to purify and filter water from unwanted substances, whether they are dyes, organic or inorganic substances, or biological waste. Choosing the required method for water treatment is subject to certain considerations, including ease of application, low financial cost, and efficiency. Removal of pollutants, including dyes, can be done by the adsorption process due to the ease of applying this process, its low cost, its high efficiency, its high selectivity, wide range of impurities that can be removed, ease of obtaining adsorbent materials, and the absence of leaving harmful environmental residues through its reactivation. Solid adsorbent surfaces, whether organic, inorganic, or polymeric, used to adsorb the desired molecules are available in abundance and of different types⁽⁶⁾. The principle of adsorption theory and method is based on adhesion of molecules or atoms of the adsorbate material, whether liquid or gaseous, to the solid adsorbent material⁽⁷⁾. This adhesion takes place between both adsorbate molecules on the surfaces and through the pores of the adsorbent material unless the adsorption is single-layer or multi-layer. Adsorption can be classified based on the nature of association between each of molecules of adsorbate and adsorbent surface⁽⁸⁾. On this basis, there are two main types of adsorptions. Physical adsorption, in which the nature of connection between adsorbate and adsorbent material is through weak Vander Waals forces, or connection is through strong chemical bonds, so name of this type is chemical adsorption⁽⁹⁾. What distinguishes physical adsorption is that it does not require a high activation energy, and the relatively weak Wander Waals forces make it a reversible adsorption, meaning that adsorbed material can be separated from adsorbent material by controlling the process conditions of temperature and pressure,

and it is classified as multi-layer adsorption. Chemical adsorption is characterized by strength of the bonds that form in form of chemical bonds between adsorbed molecules and adsorbent, which cannot be broken easily⁽¹⁰⁾. Therefore, it is classified as a single-layer irreversible adsorption and requires a relatively higher activation energy. This type of adsorption has a wide range of selectivity. Aim of study prepare of (Magnesium borate) and study it is ability to act as photocatalyst to remove CR dye from aqueous solution by adsorption method .

2.Methods

2.1. Preparing Adsorbent

Magnesium borate was synthesized by one-single step precipitation by mixing magnesium oxide NP and boric acid with molar ratio (2:1), in 200 ml distilled water under stirrer 500 rpm at mixing time 10 hours at (60 °C), after that the mixture was filtered, then washed for several time with distilled water to remove the excess of boric acid. The product dried in oven for 24 hours at 70 °C⁽¹¹⁾.

2.2. Preparing Adsorbate

Congo Red dye solution was prepared by dissolving 1 g of dye in a 1000 ml of distilled water, after that different concentrations of dye were prepared.

2.3 Photocatalyst process

A different concentration of dye was prepared at pH (5.5) and at required temperature and placed in a test tube after that adsorbent (MB) loaded with weight (0.1) g, then placed in shaker and exposed to sunlight for interval time, then centrifuged to separate the aqueous solution and measured at wavelength of 495 nm.

3.Results and discussion

3.1. Characterization of prepared

3.1.1 FTIR analysis

FT-IR spectra shown in Figure 1 absorption peak was observed at 3576 cm⁻¹ due to (O-H) band of water, two absorption peaks were observed at 1496 cm⁻¹ and 1273 cm⁻¹, the peaks were arisen because of the asymmetric stretching of the three-coordinate

boron to oxygen bands (B(3)-O). The peak at 1100 cm⁻¹ might be due to bending of boron-oxygen-hydrogen (B-O-H). The presence of IR peaks between 972 cm⁻¹ and 820 cm⁻¹ revealed the symmetric stretching of the three-coordinate boron to oxygen bands (B(3)-O). Also, the peak below 563 cm⁻¹ was due to the symmetric stretching of the four-coordinate boron to oxygen bands (B(4)-O) and the peak below 413 cm⁻¹ was due to (Mg-O) band ⁽¹²⁾.

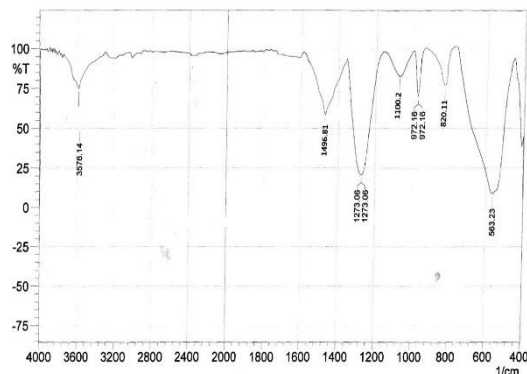


Figure 1: FTIR spectrum of (MB)

3.1.2 X-Ray diffraction (XRD)

XRD pattern of (MB) shown in Figure 2. Values of (2θ) for main peaks of Magnesium borate were reported as (15°, 20.0°, 22.0°, 27°, 28.3°, 29.0°, 30°, 32.5°, 35.2°, and 42.7°). 2θ values of XRD patterns of solid products are determined as which are completely consistent with XRD pattern given in results of research Paper ⁽¹³⁾. Average crystallites size in (44.39) nm as calculated from Scherrer equation . that crystals of the compound fall within nanoscales .

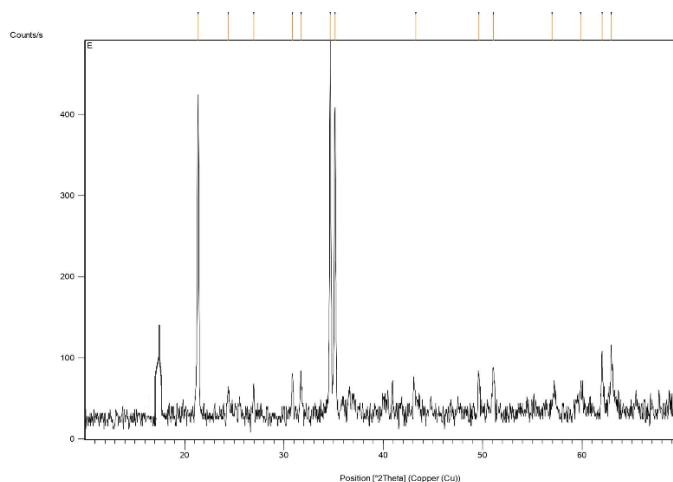


Figure 2: XRD spectrum of (MB) surface

3.1.3 Scanning Electron Microscopy (SEM)

The shapes represent the images of the scanning electron microscope with a field of light emission of the prepared compound, the images of the compound showed the shape of its Shell-shaped surface, the compound contains holes and pores, and that presence of these pores increases surface area of compound and therefore these holes will play an important role in increasing adsorption process⁽¹⁴⁾.

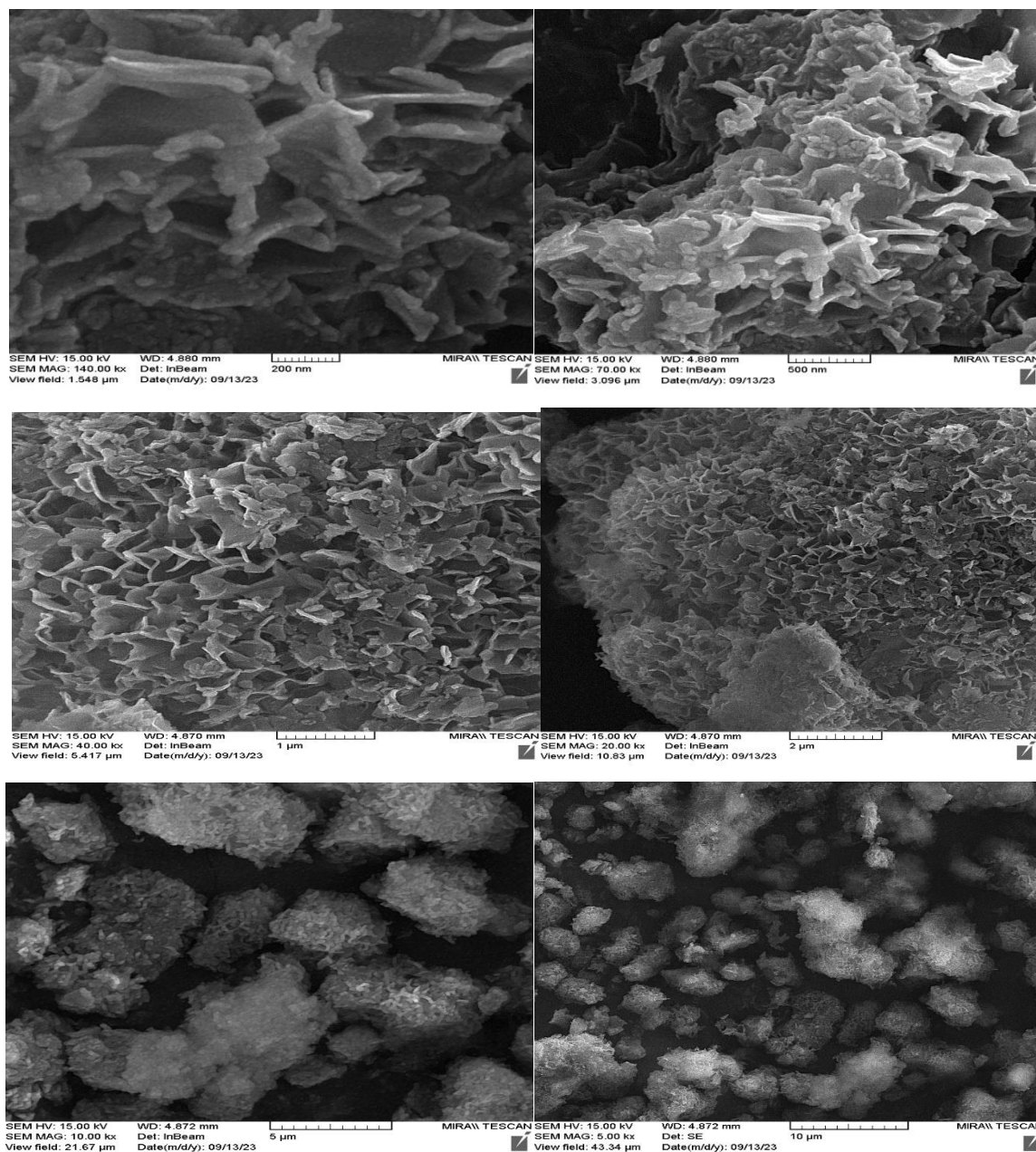


Figure (3) SEM of (MB) in different dimension

3.1.4 Energy Dispersive X-rays Analysis (EDX)

EDX analysis of (MB) as shown in Table 1 and Figure 4. Percentage weight composition of (MB) is Magnesium 30.03%, oxygen 64.39%, and boron 5.58%. The chemical composition of (MB) sample was determined as Mg: 21.39%, O: 69.68%, and B: 8.93

% using data in EDS analysis. While experimental and theoretical composition value of Mg and O are close to each other, the value of B is completely different as boron element has low atomic mass⁽¹⁵⁾ .

Table (1) EDX values of (MB) composition.

Composition	W%	A%
B	5.58	8.93
O	64.39	69.68
Mg	30.03	21.39
Total	100.00	100.00

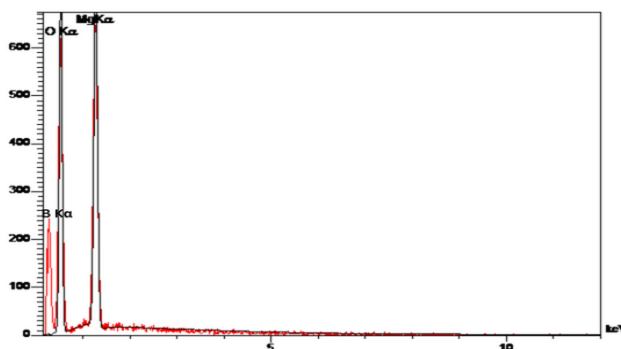


Figure (4) EDX positions of (MB) compound

3.1.5 Zeta Potential analysis

There are many different ways of calculating zeta potential. In this study, method of calculating zeta potential in electrophoretic.

Table (2) explain range of stability according to Zeta potential.

Stability behavior of the particles	Zeta Potential (mV)
Rapid Coagulation or Flocculation	0 to ± 5
Incipient Instability	± 10 to ± 30
Moderate Stability	± 30 to ± 40
Good Stability	± 40 to ± 60
Excellent Stability	More than ± 61

As shown in Figure 5 and Table 3 value of zeta potential of (MB) (-39.7 mv) and that is mean the surface of product has negative charge, and it is stable, and it is good to use to adsorb CR from aqueous solution⁽¹⁶⁾. (MB) product it is too difficult to make colloid with solution so that it easy to isolate it from aqueous solution to measure amount of adsorption.

Table (3) Zeta potential value of (MB).

Peak NO:	zeta potential	Electrophoretic
1	-39.7 mV	- 0.000206 cm ² /Vs

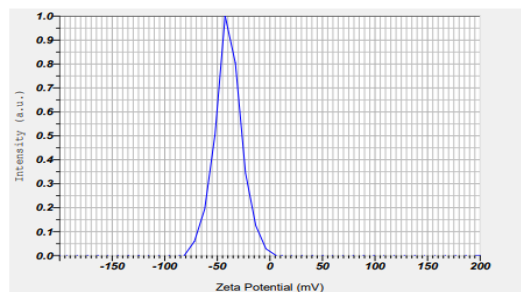


Figure (5) Zeta potential position of (MB) surface

Determination the calibration curve.

Standard curve of dye was calculated by preparing different concentrations 5,10,15,20, 25 ppm at pH = 8 and the absorption was measured at the highest wavelength 495 nm by plotting concentration versus absorption, where $R^2 = 0.9973$ represents the linear equation as in Figure 6.

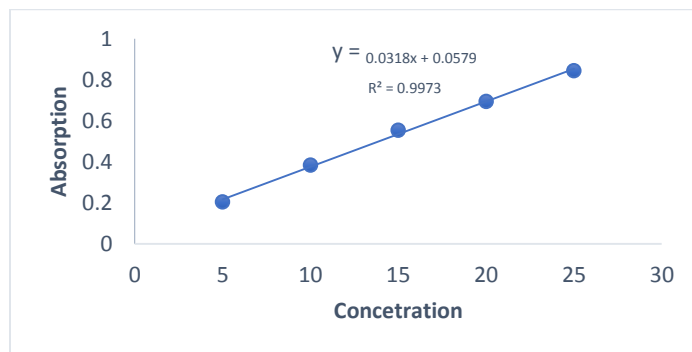


Figure (6) calibration curve of CR dye.

4. Adsorption studies

4.1. Study of adsorption time Equilibrium

The factor affecting of adsorption efficiency is the equilibrium time between adsorbent (MB) and CR dye⁽¹⁷⁾. Using a weight of 0.1 gm with a dye concentration 25 ppm at a temperature 300⁰K at different times within the range 1-100 min, as the results shown in Figure 7 and Table 4 show that time of 30 min is best equilibrium time for adsorption process.

Table (4) time Equilibrium of adsorption CR dye on (MB) surface

(q) mg/g	11.96	15.31	17.57	18.42	19.17	19.30
Time (min)	5	10	15	30	45	60

$$q = \frac{(C_o - C_e)V}{M}$$

q: Amount of adsorbate on (MB) surface in (mg/g)

were

C₀: initial concentration of CR in solution

C_e: Remaining concentration of CR in solution in (mg/L)

V : Volume of solution in (L)

M: Wight of adsorbent MB in (gm)

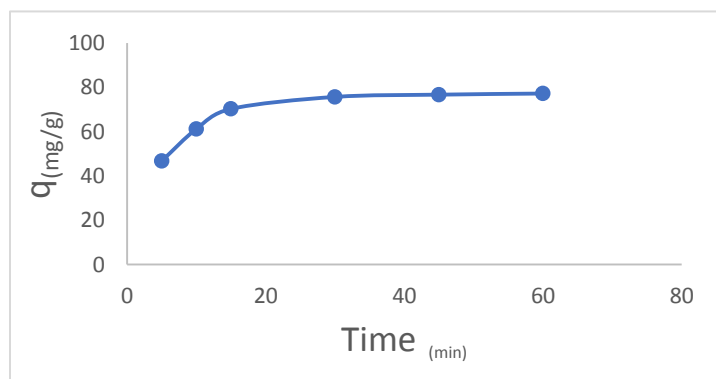


Figure (7) effect change time on adsorption process.

4.2 Study of factors affecting the removal of CR dye from aqueous solutions using (MB) as adsorbent surfaces

4.2.1 Effect of adsorbent weight

Effect of altering weight of adsorbent on adsorption of red Congo dye was studied using a weights (0.1,0.02,0.03,0.06) g and at times up to 60 min and dye concentration at 25 ppm and volume 100 ml and wavelength (495 nm) It was found that adsorption increases with increase catalyst weight due to increase in surface area that provides greatest value for active areas⁽¹⁸⁾ as shown in Table 5 and Figure 8.

Table (5) effect change weight of (MB) surface on adsorption process.

Weight (g)	0.06	0.1	0.2	0.3
q mg/g	12.952	15.575	23.896	24.808

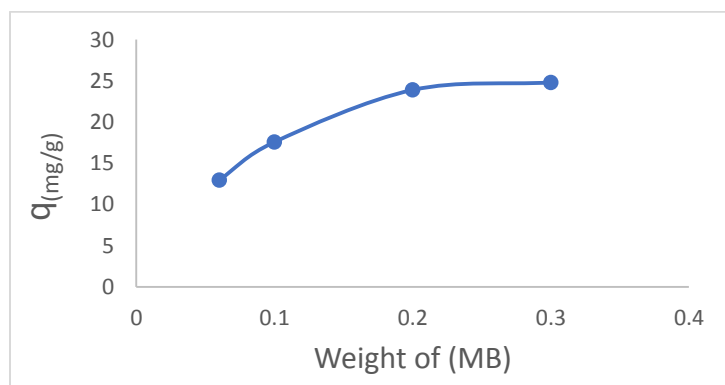


Figure (8) effect change weight of (MB) adsorbent on adsorption process.

4.2.2 Effect of pH

Removal percentage of CR dye using 0.1 g of (MB) in 100 ml with 25 ppm at time 60 min with different pH 3,5,7,9 and 11 adsorption of dye in acidic medium is greater than in base medium as shown in Table 6 and Figure 9, that is, ability of dye tendency to bind in acidic medium with the catalyst is more than its tendency to bind with solvent molecules, since the process of remove dye by photocatalysis is subject to several mechanisms, including direct reduction by electrons in the conduction beam, direct

oxidation through gaps in the valence beam, and finally hydroxyl radical attack⁽¹⁹⁾. These mechanisms mentioned depend on nature of the material and pH function of medium in which adsorption process takes place has an effect on both adsorbate and adsorbent. but it should be noted that this dye is deposited at pH=2 and also changes the color of dye at acid function pH=3 causing a difference in wavelength, so it was settled to use value of pH = 5.5 in next experiments.

Table (6) Effect pH on adsorption process.

pH	3	5	7	9	11
(q)	24.776	15.845	14.116	10.562	11.5069

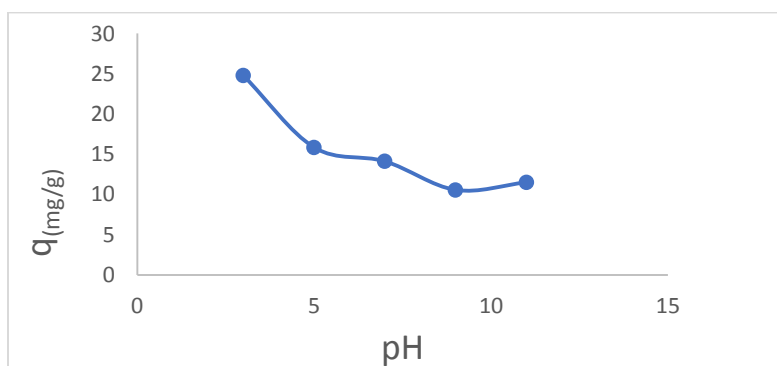


Figure (9) effect change pH solution on adsorption process.

4.2.3 Effect of the initial dye concentration

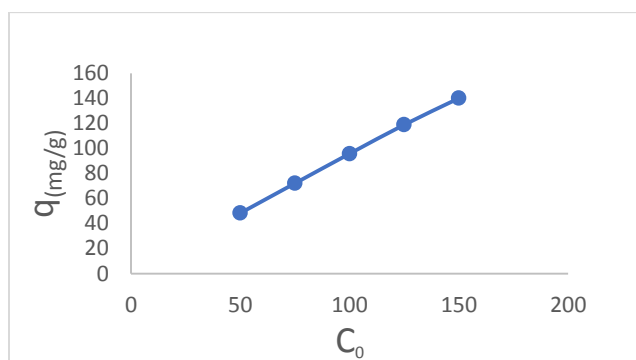
Altering concentration of dye effect on adsorption process, it is one of important factors, so in this study different concentrations of CR dye were taken. Values 50,75,100,125 and 150 ppm with a constant weight of adsorbent of Magnesium borate, increase in adsorption efficiency was observed with increase concentrations of dye where highest adsorption value was recorded⁽²⁰⁾, as shown in Table 7 and Figure 10 this is due to fact that largest amount of dye will be adsorbed on adsorbent and thus generation of free radicals for hydroxyl will decrease due to lack of active sites of hydroxyl ions, noting a decrease in percentage of adsorption in high initial concentration of dye, which hinders access of photons of light to the catalytic surface causing a decrease in absorption of photons, consequently a decrease in decomposition rate.

Table (7) Effect of Initial dye Concentration On adsorption process.

C_0	50 ppm	75 ppm	100 ppm	125 ppm	150 ppm
q	48.424	72.166	95.814	118.928	140.06

Table (8) maximum adsorption amount of CR dye at maximum concentration on (MB) surface

Adsorbent	(MB)
Concentration	150
q	140.06

**Figure (10) effect change of Initial dye Concentration on adsorption process.**

4.2.4 Effect of Temperature

Temperature of medium that occurs when adsorption is one of the factors effecting on removal dye, in this study measurements were made within three temperatures (300^0K , 318^0K and 333^0K) where it was found that efficiency of adsorption increases with increasing temperature degree and accelerates access to equilibrium time⁽²¹⁾, where measurements made at a constant concentration and different times extended from (5-90 min), also weight of adsorbent used to adsorb CR dye was constant 0.1 g, increasing efficiency of adsorption due to obstruction of rearrangement electron - gap process due to increasing temperature, and this cycle proves that the adsorption process on this adsorbent is an endothermic process, in addition to that high temperature increases rate of oxidation of organic compounds and thus enhances decomposition capacity. As shown in Table 9 and Figure 11.

Table (9) Effect of Change temperature on adsorption process.

Time (MB)	300 K		318 K		333 K	
	C_e	q	C_e	q	C_e	q
5	23.14	26.852	29.675	20.342	22.33	27.66
10	18.27	31.726	20.820	29.179	17.89	32.10
15	12.95	37.040	8.2421	41.757	2.455	47.54
30	5.663	44.336	2.2358	47.764	1.323	48.67
45	2.361	47.638	1.0408	48.959	1.198	48.80
60	2.141	47.858	0.8836	49.116	1.198	48.80

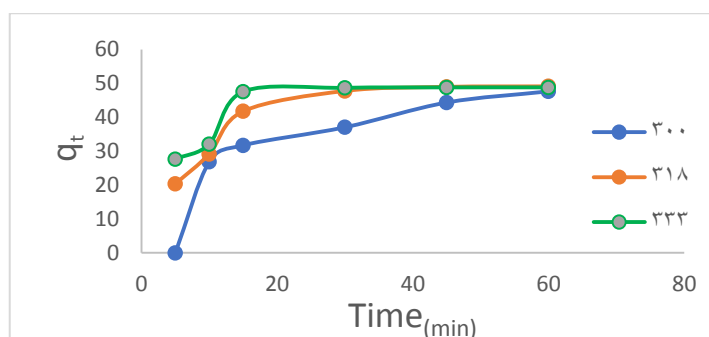


Figure (11) effect change of temperature on adsorption of CR dye.

5 Adsorption Isotherm

Calculations and study of adsorption isotherm, calculations of effect primary dye concentration at room temperature 300^0K was used to apply mathematical equation of isotherm Langmuir by plotting linear equation of Langmuir equation based on values of C_e and C_e/q_e as shown in Table 10 and Figure 12. Langmuir constant (K_L), values of maximum adsorption (Q_{max}) and correlation coefficient (R^2) were calculated, and these values are shown in Table 11.

Table (10) Langmeyer isotherm study on adsorption amount of CR dye on (MB) adsorbent in (mg/g).

C_0	C_e	q_e	C_e/q_e
50 ppm	1.575	48.424	0.0325
75 ppm	2.833	72.166	0.0392
100 ppm	4.185	95.814	0.0436
125 ppm	6.072	118.928	0.0510
150 ppm	9.940	140.06	0.0709

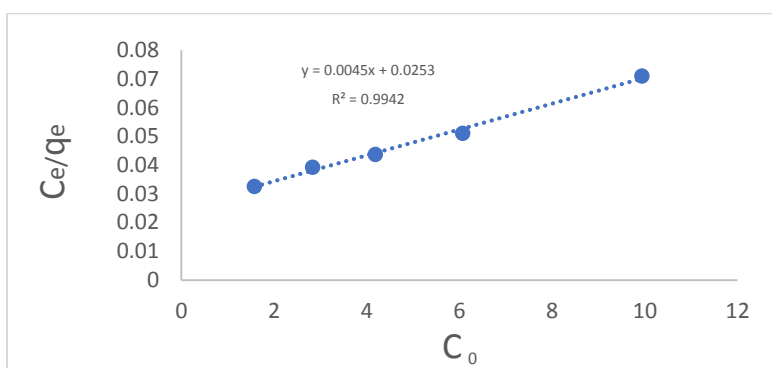


Figure (12) shown Langmeyer adsorption Isotherm of CR dye.

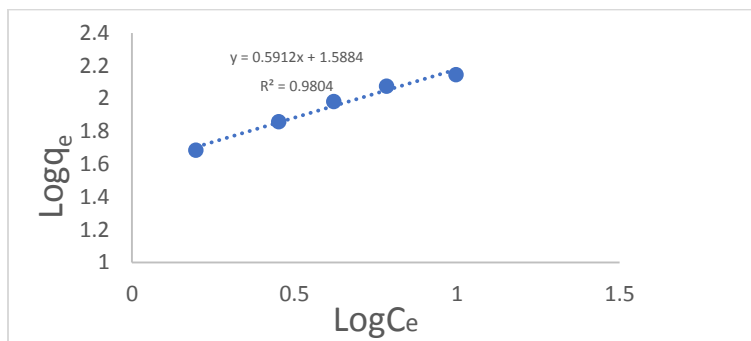
Table (11) The Langmeyer constant (K_L), the value of the maximum adsorption (Q_{max}) and the correlation coefficient (R^2)

Compound	q_{max}	K_L	R^2
(MB)	222.2	0.1778	0.9942

Linear relationship of Freundlich equation was plotting based on values of $\log C_e$ versus $\log q_e$ shown in Table 12 and Figure 13. Values of Freundlich constants (R^2, n, K_f) shown in Table 13 .

Table (12) Freundlich's adsorption Isotherm

C_0	50	75	100	125	150
Log C_e	0.197	0.452	0.621	0.783	0.997
Log q_e	1.685	1.858	1.981	2.07252	2.146

**Figure (11) Freundlich's adsorption Isotherm of CR dye.****Table (13) Freundlich's adsorption Isotherm values**

Compound	Temp	n	K_f (mg/g)	R^2
(MB)	300 k	1.69	4.8959	0.9804

value ($R^2 = 0.9942$) of Langmuir isotherm and ($R^2 = 0.9804$) value of Freundlich Isotherm so that adsorption process flowing (Langmeyer isotherm model)

4. Thermodynamic study (calculation of thermodynamic functions).

Through courante study effect of change temperature on adsorption process, this helped to calculate thermodynamic functions (ΔH enthalpy, ΔG free energy and ΔS entropy). For adsorption of red Congo dye on adsorbent of (MB) importance of these functions to understanding adsorption process. Table 14 represents values of both $\ln k_c$ and values of temperature, while Figure 14 represents relationship between $\ln K_c$ versus inverse of time ($1/T$), from which values of (ΔH , (ΔS) can be obtained that can be calculated through values of interception = ($\Delta H/R$) and slop = ($\Delta S/R$), Table 15 shown thermodynamic values.

Table (14) values of both (Ln kc) and the values of Inverse temperature

T(K ⁰)	300	318	333
1/T * 10 ⁻³	3.333	3.144	3.003
ln K _c	2.058	3.06	3.7

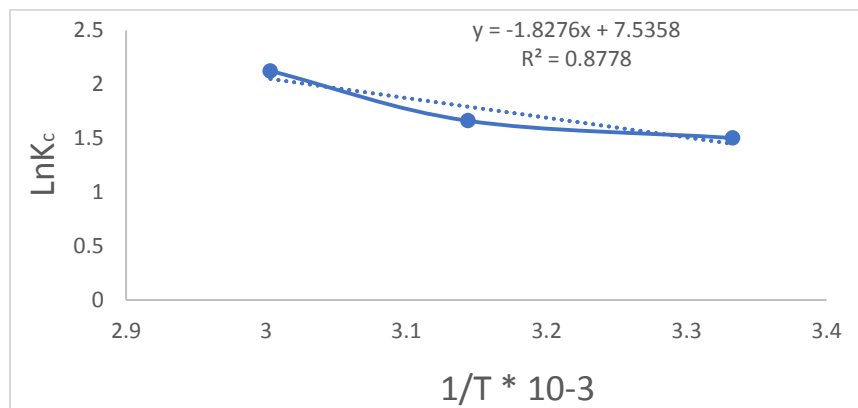


Figure (14) linear relationship between lnk_c vs. 1/T*10⁻³ to Isotherm of CR dye.

Table (15) values of (ΔH enthalpy, ΔG free energy , ΔS entropy).

Compound	ΔG(KJ.mol ⁻¹)			ΔS(KJ.K ⁻¹ .mol ⁻¹)	ΔH(KJ.mol ⁻¹)
	300	318	333		
(MB)	-(5.133)	-(8.0928)	-(10.15)	155.6	41.52

From values shown above in the Table 15 we conclude the following free energy values (ΔG) of adsorption for compound (MB) is negative, which is evidence that adsorption process is spontaneous. Entropy values (ΔS) for adsorption for compounds (MB) is positive, indicating that adsorbent molecules are in continuous motion on surface of adsorbent compounds, indicating an increase in system randomness. Values of adsorption temperature (enthalpy ΔH) are positive for adsorption of compound (MB) indicating that adsorption process is endothermic, and that increasing temperature leads to an increase in rate of propagation speed of adsorbed particles on adsorbent surface between pores in adsorbent surface.

1- False first order equation (Lagergren), where the experimental data were applied to the Lagergren Pseudo first order - equation

2- False second order equation: This equation shows that adsorption rate depends on adsorption amplitude in the adsorption surface, (Lagergren Pseudo second order – equation). Table 16 shown value of $\ln q_e - q_t$ and time values (t) of adsorption process of CR on adsorbent (MB) and Figure 13 represent the linear relationship of the false first-order equation, from which the adsorption rate constant (K_1), adsorption capacity (q_e) and the correlation coefficient shown in Table 17 were calculated.

Table (16) values of ($\ln q_e - q_t$) versus time values (t) of adsorption process

Time	5	10	15	30	45	60
q_e	26.852	31.726	39.210	44.336	47.638	49.525
t/q_t	0.1862	0.3151	0.3825	0.6766	0.9446	1.2115
$\ln(q_e - q_t)$	3.796	3.676	3.541	2.971	1.509	NUM

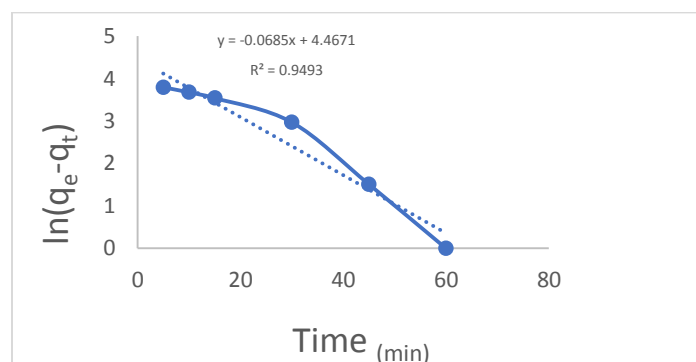
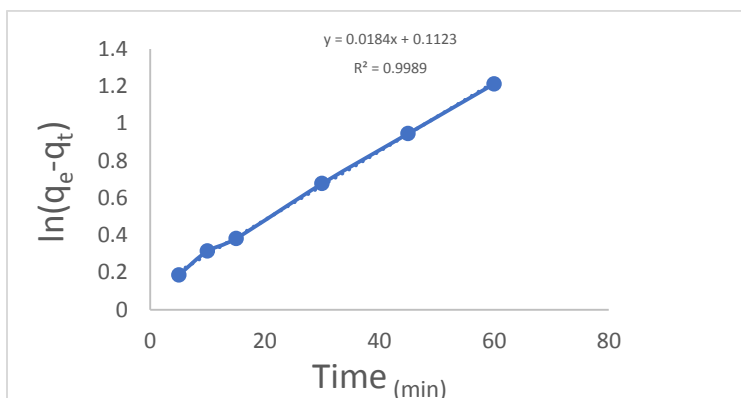


Figure (13) represent the linear relationship of the false first-order equation.

Table (17) Value False first order equation (Lagergren)

Compound	$Q_{e, \text{exp}}$	$k_1(\text{min}^{-1})$	q_e (mg/g)	R^2
(MB)	42.732	0.00146	8.483	0.9493

**Figure (14) represent linear relationship of the false second-order equation.****Table (18) Value False second order equation**

Comp	$Q_{e, \text{exp}}$	$k_2(\text{min}^{-1})$	q_e (mg/g)	R^2
(MB)	49.252	0.003015	54.34	0.9989

From values in Table 17 and Table 18 it is clear that the process of adsorption of CR dye on surface (MB) follows the second kinetic equation for the following reasons, the large difference between values of adsorption capacity calculated according to the false first order equation ($q_{e(\text{calculated})}$) is different from the experimental adsorption value ($q_{e(\text{experimental})}$) obtained through this study, through the Figures, the linear axis of false first-order equation does not pass through all points, unlike the linear axis of the false second-order equation, which passes exactly all points. the correlation values (R^2) of the false first order equation (0.9493) is less than away from the value of (1) unlike the correlation values (R^2) of the false second-order equation, which is limits (0.9989) near to (1).

Conclusions

(MB) Successfully synthesized by one step precipitation from nano Magnesium oxide and amount of Boric acid. FTIR analysis the locations of the active aggregates of the compound were clearly shown. XRD analysis the position 2θ for crystal lattice patterns clarified the dimensions and size of the crystal. SEM analysis the images showed surface of the compound contains holes and pores. EDS analysis prove that solid product compound obtained. Zeta potential analyses we note value of zeta potential of (MB) has negative charge. All conditions effect on adsorption process have been study also isotherm and the process following Langmeyer isotherm and kinetic have been explained and the adsorption process following second order equation .

الاستنتاجات

تم بنجاح تحضير بورات المغنسيوم النانوية بالطريقة الحرارية المائية و بخطوة ترسيبية واحدة من خلال تفاعل اوكسيد المغنسيوم النانوي مع حامض البوريك. تم تشخيص المركب بمطيافية الاشعة تحت الحمراء و التي اظهرت المواقع الفعالة للمركب التي تتطابق مع ظروف تفاعل التحضير من درجة حرارة و ضغط و حامضية . مطيافية الاشعة السينية المشتتة اظهرت مواقع (2 theta) التي فسرت بنية الخلية للبلورة . صور المجهر الالكتروني الماسح بينت بوضوح وجود مسامات و فجوات مناسبة الحجم لامتماز صيغة الكونغو الاحمر من محلولها المائي . مطيافية الطاقة المشتتة بين النسب المئوية للعناصر الرئيسية المكونة للمركب حيث كانت النتائج بالقيم المطلوبة . قياس طاقة زيتا لسطح المركب كشف ان الشحنة للسطح هي سالبة و التي تفسر سبب عملية الامتماز. جميع الظروف التي تؤثر على عملي الامتماز تم دراستها كذلك حركية الامتماز و نوعية.

References

- [1] Prasad, S. S., Prasad, S. B., Verma, K., Mishra, R. K., Kumar, V., & Singh, S. (2022): The role and significance of Magnesium in modern day research-A review. Journal of Magnesium and Alloys. **10(1)**, 1-61.
- [2] Wang, X., Pang, H., Chen, W., Lin, Y., Zong, L., & Ning, G. (2014): Controllable fabrication of zinc borate hierarchical nanostructure on brucite surface for enhanced mechanical properties and flame-retardant behaviors. ACS Applied Materials & Interfaces. **6(10)**, 7223-7235.

- [3] Jagtap, A., Wagle, P. G., Jagtiani, E., & More, A. P. (2022): Layered double hydroxides (LDHs) for coating applications. *Journal of Coatings Technology and Research*. **19(4)**, 1009-1032.
- [4] Dwivedi, P. B., & Retna, M. (2015): *Book of Proceedings*.
- [5] Raval, N. P., Shah, P. U., & Shah, N. K. (2016): Adsorptive amputation of hazardous azo dye Congo red from wastewater: a critical review. *Environmental Science and Pollution Research*. **23**, 14810-14853.
- [6] Awad, A. M., Jalab, R., Benamor, A., Nasser, M. S., Ba-Abbad, M. M., El-Naas, M., & Mohammad, A. W. (2020): Adsorption of organic pollutants by nanomaterial-based adsorbents: An overview. *Journal of Molecular Liquids*. **301**, 112335.
- [7] Pourhakkak, P., Taghizadeh, A., Taghizadeh, M., Ghaedi, M., & Haghdoost, S. (2021): Fundamentals of adsorption technology. In *Interface Science and Technology*. **33**, 1-70.
- [8] Al- Wasidi, A. S., AlZahrani, I. I., Naglah, A. M., El- Desouky, M. G., Khalil, M. A., El- Bindary, A. A., & El- Bindary, M. A. (2021): Effective removal of methylene blue from aqueous solution using metal- organic framework; modelling analysis, statistical physics treatment and DFT calculations. *Chemistry Select*. **6(41)**, 11431-11447.
- [9] Tomul, F., Arslan, Y., Kabak, B., Trak, D., & Tran, H. N. (2021): Adsorption process of naproxen onto peanut shell- derived biosorbent: important role of $n-\pi$ interaction and van der Waals force. *Journal of Chemical Technology & Biotechnology*. **96(4)**, 869-880.
- [10] Ammendola, P., Raganati, F., & Chirone, R. (2017): CO₂ adsorption on a fine activated carbon in a sound assisted fluidized bed: Thermodynamics and kinetics. *Chemical Engineering Journal*, **322**, 302-313.

- [11] Shah, F. U. (2011). Designed boron chemistry for tribological systems (Doctoral dissertation, Luleå tekniska universitet).
- [12] Stanzione III, J. F., Giangiulio, P. A., Sadler, J. M., La Scala, J. J., & Wool, R. P. (2013): Lignin-based bio-oil mimic as biobased resin for composite applications. *ACS Sustainable Chemistry & Engineering*, **1(4)**, 419-426.
- [13] Bai, M., Hu, L., Liang, Y., Hong, B., & Lai, Y. (2021): Enhanced Electrochemical Properties of Lithium- Rich Cathode Materials by Magnesium Borate Surface Coating. *Chemistry Select.* **6(9)**, 2446-2455.
- [14] Zhu, L., Shen, D., & Luo, K. H. (2020): A critical review on VOCs adsorption by different porous materials: Species, mechanisms, and modification methods. *Journal of hazardous materials.* **389**, 122102.
- [15] Häuser, K., Azmi, R., Agrawal, P., Jakoby, R., Maune, H., Hoffmann, M. J., & Binder, J. R. (2021): Sintering behavior and electrical properties of the paraelectric/dielectric composite system BST/MBO. *Journal of the European Ceramic Society.* **41(14)**, 7022-7028.
- [16] Oo, M. H., & Ong, S. L. (2010): Implication of zeta potential at different salinities on boron removal by RO membranes. *Journal of membrane science.* **352(1-2)**, 1-6.
- [17] Rápó, E., & Tonk, S. (2021): Factors affecting synthetic dye adsorption; desorption studies: a review of results from the last five years (2017–2021). *Molecules.* **26(17)**, 5419.
- [18] Leofanti, G., Padovan, M., Tozzola, G., & Venturelli, B. J. C. T. (1998): Surface area and pore texture of catalysts. *Catalysis today.* **41(1-3)**, 207-219.
- [19] Chatterjee, D., Dasgupta, S. (2005): Visible light induced photocatalytic degradation of organic pollutants. *Journal of Photochemistry and Photobiology C: Photochemistry Reviews.* **6(2-3)**, 186-205.

- [20] Garg, V. K., Kumar, R., Gupta, R. (2004): Removal of malachite green dye from aqueous solution by adsorption using agro-industry waste: a case study of *Prosopis cineraria*. *Dyes and Pigments*. **62(1)**, 1-10.
- [21] Ghaedi, M., Sadeghian, B., Pebdani, A. A., Sahraei, R., Daneshfar, A., & Duran, C. E. L. A. L. (2012): Kinetics, thermodynamics, and equilibrium evaluation of direct yellow 12 removal by adsorption onto silver nanoparticles loaded activated carbon. *Chemical Engineering Journal*. **187**, 133-141.